Acta Polytechnica **65**(2):237–242, 2025
https://doi.org/10.14311/AP.2025.65.0237

URANIUM FOIL NEUTRON ACTIVATION ANALYSIS

Ján Kozic[a, b, *], Milan Štefánik[a, b]

[a] *Czech Technical University in Prague, Faculty of Nuclear Sciences and Physical Engineering, Department of Nuclear Reactors, V Holešovičkách 2, 180 00 Prague, Czech Republic*

[b] *Czech Academy of Sciences, Nuclear Physics Institute, Řež 130, 250 68 Řež, Czech Republic*

[*] corresponding author: kozicjan@cvut.cz

Abstract. At the Department of Nuclear Reactors of the Faculty of Nuclear Sciences and Physical Engineering of the Czech Technical University (FNSPE CTU) in Prague, there is a need to implement a neutron activation analysis as a tool for the separation of uranium foils depending on various ^{235}U and ^{238}U contents. Experiments were carried out on the training reactor VR-1 "Sparrow", which is operated at the institute mentioned above. The uranium foils were analysed using the neutron activation analysis and gamma-ray spectrometry, and were separated into two groups, the first group contained foils of depleted uranium and the other contained natural uranium foils. The uranium foils can be further used for educational purposes or experimental applications, such as the measurement of neutron spectral indexes, neutron activation analysis of uranium ore, or delayed neutron analysis. The neutron activation analysis has been extended to determine whether foils contain natural or depleted uranium.

Keywords: Production rate, uranium foils, neutron activation analysis, gamma-ray spectrometry, Training Reactor VR-1, HPGe detector.

1. Introduction

Neutron activation analysis can be used as a powerful non-destructive tool for the composition analysis of investigated samples. It can be used in various nuclear facilities, such as nuclear reactors, nuclear generators, or accelerator-driven neutron sources.

The low-power reactor VR-1 "Sparrow" [1] has been operated at the Department of Nuclear Reactors of the Faculty of Nuclear Sciences and Physical Engineering of the Czech Technical University (FNSPE CTU) in Prague [2] since 1990 [1]. Its main purpose is to educate students, however, it can also be used to train qualified personnel or conduct research [1]. Various experimental equipment is available at the VR-1 reactor which allows its utilization for experimental tasks such as neutron activation analysis [3–7] or neutron radiography [8].

There is a long-standing neutron activation analysis program at the institute mentioned above [3–7]. This paper deals with the neutron activation analysis of uranium foils and is focused on an extension of the neutron activation analysis to determine whether foils contain natural or depleted uranium. The goal of this research is both the extension of the neutron activation analysis mentioned above and the separation of uranium foils depending on various ^{235}U and ^{238}U contents.

There are multiple studies considering the determination of uranium concentration based on the neutron activation analysis measurements, e.g. [9–13]. All the research mentioned measures uranium concentration based on the neutron activation of ^{238}U. Even though the studies analyse the uranium concentration, none consider uranium's isotopic composition. The need of the Department of Nuclear Reactors is to separate the uranium foils depending on various ^{235}U and ^{238}U contents, therefore, the NAA of uranium contents needs to be further extended to be able to determine whether the uranium foils are made from depleted or natural uranium.

2. Materials and methods

2.1. Neutron activation analysis

Neutron activation analysis is an experimental method which is used for qualitative and quantitative examination of the composition of an unknown sample [14]. The sample is irradiated in a well-described neutron field and then a gamma-ray spectrometry method is employed for further analysis. The qualitative examination means that the composition of the sample is determined from the measured gamma-ray spectrum via identification of the characteristic gamma radiation of the irradiated sample and further traction of reaction channels based on the energy distribution of the neutron field in which was the sample irradiated. Light water or pool-type training or research reactors have well-moderated neutron energy spectrum in specific positions of the reactor core, therefore, the radiative capture dominates as the reaction channel and the determination of the composition of the sample becomes quite certain [15].

Often there is a need to analyse quantitatively a particular element, therefore, a production rate is introduced by equations [15]:

$$P_\mathrm{R} = \frac{S(E_\gamma)\lambda\frac{t_\mathrm{real}}{t_\mathrm{live}}}{I_\gamma(E_\gamma)\varepsilon_\gamma(E_\gamma)(1-e^{-\lambda t_\mathrm{irr}})e^{-\lambda t_\mathrm{cool}}(1-e^{-\lambda t_\mathrm{real}})}, \quad (1)$$

$$P_\mathrm{R} = N_0 \int_0^{+\infty} \phi(E)\sigma(E)\mathrm{d}E, \quad (2)$$

where

$S(E_\gamma)$ is an area under the peak of full absorption in the measured gamma spectra,

λ is a decay constant of the produced nuclide,

t_live is the duration of the gamma spectrum measurement,

t_real is the duration of the gamma spectrum measurement with addition of a dead time,

$I_\gamma(E_\gamma)$ is an intensity of the particular gamma radiation,

$\varepsilon_\gamma(E_\gamma)$ is a detection efficiency of an apparatus for the particular gamma radiation,

t_irr is the duration of the irradiation,

t_cool is the cooling time,

N_0 is a number of stable nuclei in the sample,

$\phi(E)$ is a spectral neutron flux density,

$\sigma(E)$ is microscopic cross section of the particular reaction.

From a combination of the Equations (1) and (2) an expression for the number of neutral nuclei in the sample N_0 could be derived:

$$N_0 = \frac{\frac{S(E_\gamma)\lambda\frac{t_\mathrm{real}}{t_\mathrm{live}}}{I_\gamma\varepsilon_\gamma\left(1-e^{-\lambda t_\mathrm{irr}}\right)e^{-\lambda t_\mathrm{cool}}\left(1-e^{-\lambda t_\mathrm{real}}\right)}}{\int_0^{+\infty}\phi(E)\sigma(E)\mathrm{d}E}, \quad (3)$$

$$N_0 = \frac{mN_\mathrm{A}}{M_\mathrm{M}}, \quad (4)$$

where

m is a weight of the analysed nuclide,

N_A is an Avogadro's number,

M_M is a molar weight of the analysed nuclide.

A combination of the Equations (3) and (4) gives an expression for the determination of the weight of the analysed nuclide m.

Usually the information about the neutron field is not available, therefore, a comparative neutron activation analysis is introduced. In this method, an unknown sample and a standard is irradiated using the same experimental arrangement. Then a fraction of production rate of the unknown sample $P_\mathrm{R,\,sample}$ and the standard $P_\mathrm{R,\,standard}$ is analysed. For example, the weight of the observed nuclide in the unknown sample could be determined from the fraction mentioned above and the weight of the observed nuclide in the standard by an expression [15]:

$$m_\mathrm{sample} = \frac{P_\mathrm{R,\,sample}}{P_\mathrm{R,\,standard}} \cdot m_\mathrm{standrad}. \quad (5)$$

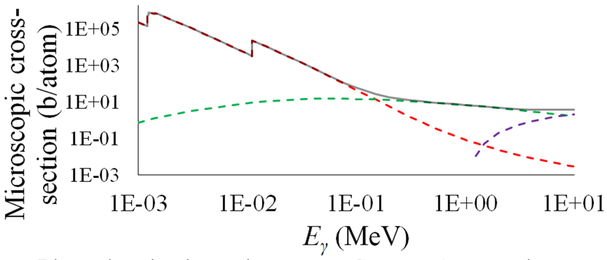

Figure 1. Microscopic cross sections for the most important interactions of the gamma radiation with germanium [16].

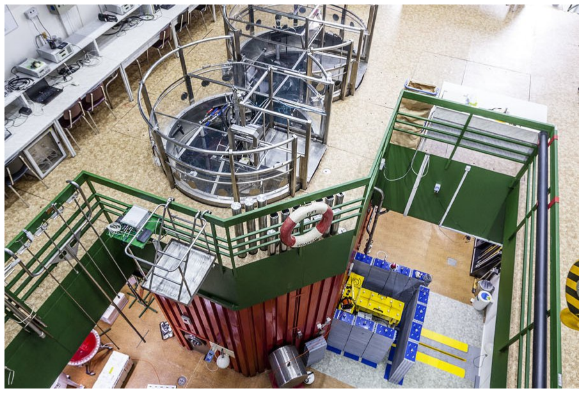

Figure 2. The Training Reactor VR-1 hall [22].

2.2. Gamma-ray spectrometry

The gamma-ray spectrometry is a method which is used for a qualitative and quantitative analysis of the gamma radiation. The qualitative analysis means the identification of the gamma radiation and the quantitative analysis stands for a counting of the identified detected gamma photons by a detection apparatus. The most important interactions of the gamma radiation with a matter are photoelectric absorption, Compton's scattering and electron-positron pair production. Microscopic cross sections of the gamma interactions mentioned above with germanium are illustrated in Figure 1, since germanium crystal is manufactured in HPGe detectors utilized in this research and they have an excellent energy resolution, therefore, HPGe detectors are widely used in the world. The data were obtained from online database [16–21].

2.3. Training reactor VR-1

The Training Reactor VR-1 “Sparrow” (see Figure 2) is a light water pool-type reactor with a nominal thermal power of 100 W which is from the point of view of a relatively high volume of a coolant a zero power reactor. The VR-1 reactor is used for the education of students, the training of qualified staff of the nuclear industry and experimental applications such as neutron activation analysis, neutron radiography, the development of new shielding materials or the development of an advanced nuclear fuel. For the experimental applications, the VR-1 reactor is

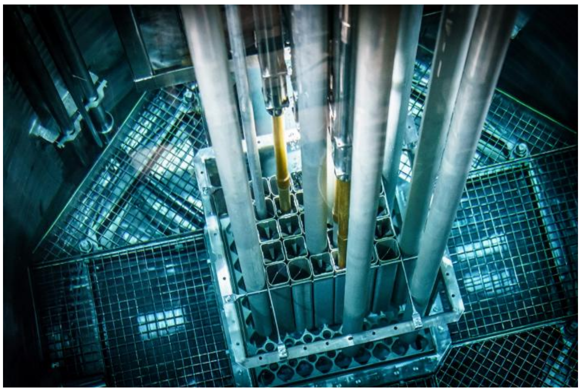

FIGURE 3. The reactor core of the VR-1 reactor [22].

equipped with various dry vertical channels, a radial and a tangential channel. The samples for the neutron activation analysis are placed into the chosen dry vertical channel. A reactor core of the VR-1 reactor is assembled on a core support plate with a square lattice of 8 × 8 cells (see Figure 3). IRT-4M nuclear fuel with ^{235}U enrichment of 19.7 % is utilized in the core. The number of fuel cells in the reactor core varies in the range from 16 to 24 depending on the actual core configuration. Absorption rods UR-70 containing a cadmium absorber are employed to control the reactor. The number of absorption rods varies in the range from 5 to 7 depending on the actual core configuration. Maximal neutron flux density reaches a value of the order $10^9\,cm^{-2}\,s^{-1}$ [1].

2.4. Data acquisition

Two experiments were carried out on the VR-1 reactor. The first and the second experiments were conducted on 2nd of June 2023 and 9th of June 2023 respectively. Totally nine uranium foils (listed in Table 1) were irradiated in a dry vertical channel on the position A4 (see Figure 4). The reactor core configuration C20 [23] was utilized and the parameters of the reactor VR-1 were the same for both of the experiments, particularly the power of the reactor reached a value of $10^7\,imp\,s^{-1}$ (ca. 10 W) and the irradiation lasted ca. 20 minutes. The foils U-dep2 and U-dep3 were utilized as standards from depleted uranium. After the irradiation, the foils were moved to a gamma-spectrometric laboratory where their gamma spectra were measured two or three times. Three semiconductor HPGe detectors Canberra [24] were employed simultaneously, therefore, even fission products with a half-life of the order of tens of minutes were measured.

3. Results

Since the fact that the analysed uranium foils have different molecular structures (U, UO_2, U_3O_8) the standard comparative neutron activation analysis for the ^{239}U to analyse ^{238}U can not be employed. However, the fraction of production rates of the unknown uranium foil and the standard could be compared to the fraction of the sum of the fission yields of ^{235}U,

Foil	Weight [mg]	Type
U-dep2	422.4	Standard
U-10	778.2	Sample
U-11	707.3	Sample
S	442.7	Sample
J	393.9	Sample
U-dep3	320.8	Standard
k0	390.5	Sample
U-1	250.4	Sample
U-X	147.3	Sample

TABLE 1. Analysed uranium foils.

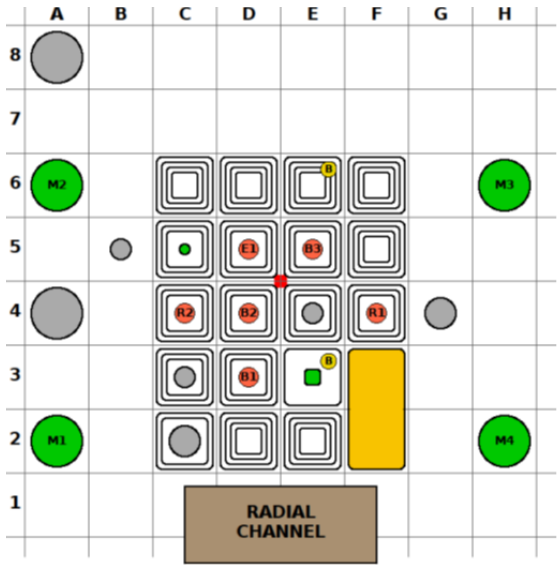

FIGURE 4. A scheme of the reactor core configuration C20 [23].

^{238}U and the fission yield of ^{238}U since the standards were made of depleted uranium. The fission products were chosen based on the following conditions:

- the yield of the fission product is higher than 5 % for ^{235}U,
- the yield of the fission product is higher for ^{235}U than for ^{238}U,
- the fission product emits gamma radiation and has a half-life such that it is possible to measure its gamma spectrum at least two times even after the necessary cooling time between the end of irradiation and the start of gamma spectra measurement.

All of the chosen fission products are summarized in Table 2 together with fission product yield for ^{235}U y_{235} and ^{238}U y_{238}, fraction $\frac{y_{238}+y_{235}}{y_{238}}$, characteristic gamma-ray energy E_γ, intensity I_γ and half-life $T_{1/2}$. The fission product yields were obtained from ENDF/B-VIII.0 nuclear database [25] and information about the gamma radiation was obtained from an online database [26].

The production rates for the chosen fission products in all of the foils were determined using Equation (1) from quantities obtained from the measured

Product	y_{238}	y_{235}	$\frac{y_{238}+y_{235}}{y_{238}}$	E_γ [keV]	I_γ [%]	$T_{1/2}$	Unit
^{142}Ba	0.09	0.15	2.74	255.30	20.50	10.60	min
^{138}Xe	0.10	0.15	2.51	258.41	31.50	14.08	min
^{101}Tc	0.12	0.14	2.15	306.86	89.00	14.22	min
^{131}Sb	0.07	0.08	2.15	943.40	47.00	23.03	min
^{146}Pr	0.06	0.08	2.38	453.88	48.00	24.15	min
^{138}Cs	0.11	0.18	2.67	1 435.80	76.30	33.41	min
^{134}Te	0.12	0.16	2.36	767.20	29.50	41.80	min
^{91}Y	0.08	0.16	3.07	555.57	95.00	49.71	min
^{134}I	0.14	0.21	2.48	847.03	95.40	52.50	min
^{97}Nb	0.11	0.18	2.62	658.08	98.00	72.10	min
^{87}Kr	0.03	0.08	3.28	402.59	49.60	76.30	min
^{139}Ba	0.11	0.18	2.64	165.86	23.70	83.06	min
^{142}La	0.09	0.16	2.80	641.29	47.00	91.10	min
^{92}Sr	0.08	0.17	3.06	1 383.93	90.00	2.71	h
^{90}Y	0.06	0.16	3.46	202.51	97.30	3.19	h
^{135}I	0.12	0.17	2.35	1 260.41	28.90	6.57	h
^{135}Xe	0.13	0.19	2.47	249.77	90.00	9.14	h
^{97}Zr	0.11	0.17	2.58	743.36	93.00	16.91	h
^{133}I	0.13	0.19	2.47	529.87	87.00	20.80	h
^{133}Xe	0.13	0.19	2.48	81.00	38.00	5.24	d

Table 2. Fission products which were chosen for analysis [25, 26].

Det.	Foil J $\frac{P_R}{P_{R,standard}}$	Foil J Result	Foil S $\frac{P_R}{P_{R,standard}}$	Foil S Result	Foil U-10 $\frac{P_R}{P_{R,standard}}$	Foil U-10 Result	Foil U-11 $\frac{P_R}{P_{R,standard}}$	Foil U-11 Result	$\frac{y_{238}+y_{235}}{y_{238}}$
DET 1	0.97	DU	1.22	DU	3.16	NU	12.28	NU	2.66
DET 2	0.92	DU	1.11	DU	11.79	NU	1.85	DU	2.61
DET 3	0.90	DU	1.07	DU	1.85	DU	1.66	DU	2.63
Result		DU		DU		NU		DU	

Table 3. Results from the first experiment.

Det.	Foil k0 $\frac{P_R}{P_{R,standard}}$	Foil k0 Result	Foil U-1 $\frac{P_R}{P_{R,standard}}$	Foil U-1 Result	Foil U-X $\frac{P_R}{P_{R,standard}}$	Foil U-X Result	$\frac{y_{238}+y_{235}}{y_{238}}$
DET 1	2.53	NU	1.23	DU	0.86	DU	2.44
DET 2	1.95	DU	1.29	DU	0.47	DU	2.76
DET 3	1.97	DU	0.78	DU	0.50	DU	2.65
Result		DU		DU		DU	

Table 4. Results from the second experiment.

gamma spectra. Then fractions of production rates of the analysed foils and the standard $\frac{P_R}{P_{R,standard}}$ were calculated. The fractions of production rates were determined for measurements on all three HPGe detectors used. The fractions of production rates were compared to the fraction of the fission product yields $\frac{y_{238}+y_{235}}{y_{238}}$. The relative difference of 20 % was allowed to determine whether the foils contain natural or depleted uranium. The results from both of the experiments are listed in Tables 3 and 4 where depleted and natural uranium are denoted as DU and NU respectively.

As a verification of the results a fraction of the production rates for the chosen fission products and production rate for ^{239}U $\frac{P_R}{P_{R,^{239}U}}$ within the analysed uranium foils were determined. Averaged values for all of the uranium foils are listed in Tables 5 and 6. The fractions for uranium foils with an unknown content of ^{238}U and ^{235}U were compared to the same fraction for the standards containing only depleted uranium. As can be seen from Tables 3, 4, 5 and 6 there is agreement in between the newly imposed methodology and the validation method.

The processing of data and its analysis is an extensive task. The preparation of data for chosen fission product measured on chosen detector for the first and the second experiment are summarized in Tables 7 and 8 respectively. The fraction $\frac{y_{238}+y_{235}}{y_{238}}$ which serves

Det.	Foil U-dep2 $\frac{P_R}{P_{R,^{239}U}}$	Foil J $\frac{P_R}{P_{R,^{239}U}}$	Foil J Result	Foil S $\frac{P_R}{P_{R,^{239}U}}$	Foil S Result	Foil U-10 $\frac{P_R}{P_{R,^{239}U}}$	Foil U-10 Result	Foil U-11 $\frac{P_R}{P_{R,^{239}U}}$	Foil U-11 Result
DET 1	0.08	0.07	DU	0.08	DU	0.22	NU	0.83	NU
DET 2	0.04	0.02	DU	0.04	DU	0.28	NU	0.03	DU
DET 3	0.08	0.08	DU	0.04	DU	0.06	DU	0.05	DU
Result			DU		DU		NU		DU

Table 5. Verification of the results from the first experiment.

Det.	Foil U-dep3 $\frac{P_R}{P_{R,^{239}U}}$	Foil k0 $\frac{P_R}{P_{R,^{239}U}}$	Foil k0 Result	Foil U-1 $\frac{P_R}{P_{R,^{239}U}}$	Foil U-1 Result	Foil U-X $\frac{P_R}{P_{R,^{239}U}}$	Foil U-X Result
DET 1	0.07	0.10	DU	0.07	DU	0.21	NU
DET 2	0.03	0.02	DU	0.05	DU	0.04	DU
DET 3	0.05	0.06	DU	0.05	DU	0.02	DU
Result			DU		DU		DU

Table 6. Verification of the results from the second experiment.

Prod.	Foil U-dep2 $\frac{P_R}{P_{R,^{239}U}}$	Foil J $\frac{P_R}{P_{R,standard}}$	Foil J $\frac{P_R}{P_{R,^{239}U}}$	Foil S $\frac{P_R}{P_{R,standard}}$	Foil S $\frac{P_R}{P_{R,^{239}U}}$	Foil U-10 $\frac{P_R}{P_{R,standard}}$	Foil U-10 $\frac{P_R}{P_{R,^{239}U}}$	Foil U-11 $\frac{P_R}{P_{R,standard}}$	Foil U-11 $\frac{P_R}{P_{R,^{239}U}}$
^{134}Te	0.12	0.97	0.13	1.22	0.14	3.16	0.22	12.28	0.83

Table 7. Data preparation from the measurement on the DET 1 for the first experiment.

Prod.	Foil U-dep3 $\frac{P_R}{P_{R,^{239}U}}$	Foil k0 $\frac{P_R}{P_{R,standard}}$	Foil k0 $\frac{P_R}{P_{R,^{239}U}}$	Foil U-1 $\frac{P_R}{P_{R,standard}}$	Foil U-1 $\frac{P_R}{P_{R,^{239}U}}$	Foil U-X $\frac{P_R}{P_{R,standard}}$	Foil U-X $\frac{P_R}{P_{R,^{239}U}}$
^{87}Kr	0.02	2.02	0.02	0.78	0.02	0.47	0.02

Table 8. Data preparation from the measurement on DET 3 for the second experiment.

as comparative condition for value of $\frac{P_R}{P_{R,standard}}$ could be found in Table 2.

4. Conclusion

In the present work, the neutron activation analysis have been extended to separate uranium foils depending on various ^{235}U and ^{238}U contents. Furthermore, the uranium foils have been separated into two groups of foils. The first group contains natural uranium foils and the other contains depleted uranium foils. The results are summarized in Tables 3 and 4. The results were verified with another method and the results of the verification method are listed in Tables 5 and 6. The verification method is in excellent agreement with the newly imposed methodology. The analysed foils can be used further in the education of students or in experimental applications such as measurements of neutron spectral indexes, neutron activation analysis of uranium ore or delayed neutron analysis. Finally, two new experimental methods for the analysis of the ^{235}U and ^{238}U contents were imposed.

The experiments are a part of the program devoted to the neutron activation analysis measurements at the Department of Nuclear Reactors of FNSPE CTU in Prague.

Acknowledgements

Research activities and irradiation experiments at the Training Reactor VR-1 were supported by the project Large Research Infrastructures (project no. LM2023073) of the Ministry of Education, Youth and Sports of the Czech Republic and the Grant Agency of the Czech Technical University in Prague, grant No. SGS23/123/OHK4/2T/14.

References

[1] Training reactor VR-1, 2017. [2024-06-17]. `https://reaktor-vr1.cz/en/about-us/{VR-1}`

[2] Czech Technical University in Prague, Department of Nuclear Reactors, 2018. [2024-06-17]. `https://katedra-reaktoru.cz/en/`

[3] M. Stefanik, S. Sazelova, L. Sklenka. Investigation of mammoth remains using the neutron activation analysis at the Training Reactor VR-1. *Applied Radiation and Isotopes* **166**:109292, 2020. `https://doi.org/10.1016/j.apradiso.2020.109292`

[4] M. Stefanik, M. Cesnek, L. Sklenka, et al. Neutron activation analysis of meteorites at the VR-1 training reactor. *Radiation Physics and Chemistry* **171**:108675, 2020. `https://doi.org/10.1016/j.radphyschem.2019.108675`

[5] M. Stefanik, J. Rataj, O. Huml, L. Sklenka. Study of dietary supplements compositions by neutron activation analysis at the VR-1 training reactor. *Radiation Physics and Chemistry* **140**:471–474, 2017. https://doi.org/10.1016/j.radphyschem.2017.03.017

[6] M. Stefanik, L. Sklenka, O. Huml, J. Rataj. Activation analysis of tibetan coins and thermal neutron flux measurement at the VR-1 training reactor. *Radiation Physics and Chemistry* **155**:304–309, 2019. https://doi.org/10.1016/j.radphyschem.2018.06.032

[7] M. Stefanik, L. Sklenka, M. Cesnek, et al. Neutron activation analysis of tibetan traditional medicinal pills at the VR-1 training reactor. *Radiation Physics and Chemistry* **167**:108554, 2020. https://doi.org/10.1016/j.radphyschem.2019.108554

[8] J. Matoušková, L. Sklenka, B. Schillinger. Investigation of Buddhist and Bon votive statues at the very low power reactor VR-1. *Nuclear Instruments and Methods in Physics Research Section A: Accelerators, Spectrometers, Detectors and Associated Equipment* **1060**:169043, 2024. https://doi.org/10.1016/j.nima.2023.169043

[9] L. Benedik, A. M. Pilar, H. Prosen, et al. Determination of ultra-trace levels of uranium and thorium in electrolytic copper using radiochemical neutron activation analysis. *Applied Radiation and Isotopes* **175**:109801, 2021. https://doi.org/10.1016/j.apradiso.2021.109801

[10] M. Byers, S. Landsberger, E. Schneider, S. Eder. Neutron activation analysis for the characterization of seawater uranium adsorbents. *Applied Radiation and Isotopes* **133**:4–8, 2018. https://doi.org/10.1016/j.apradiso.2017.11.032

[11] S. Landsberger, R. Kapsimalis. Comparison of neutron activation analysis techniques for the determination of uranium concentrations in geological and environmental materials. *Journal of Environmental Radioactivity* **117**:41–44, 2013. https://doi.org/10.1016/j.jenvrad.2011.08.014

[12] F. S. Olise, O. F. Oladejo, S. M. Almeida, et al. Instrumental neutron activation analyses of uranium and thorium in samples from tin mining and processing sites. *Journal of Geochemical Exploration* **142**:36–42, 2014. https://doi.org/10.1016/j.gexplo.2014.01.004

[13] V. Fondement, B. Perot, T. Marchais, et al. Development of a neutron probe to perform a combined measurement of uranium concentration and hydrogen porosity for mining applications. *Nuclear Instruments and Methods in Physics Research Section A: Accelerators, Spectrometers, Detectors and Associated Equipment* **1059**:168888, 2024. https://doi.org/10.1016/j.nima.2023.168888

[14] Z. B. Alfassi. *Activation analysis*. Volume I. CRC Press, 1990. ISBN 0-8493-4583-9.

[15] R. R. Greenberg, P. Bode, E. A. De Nadai Fernandes. Neutron activation analysis: A primary method of measurement. *Spectrochimica Acta Part B: Atomic Spectroscopy* **66**(3–4):193–241, 2011. https://doi.org/10.1016/j.sab.2010.12.011

[16] National Institute of Standards and Technology. NIST XCOM: Element/compound/mixture. [2024-06-17]. https://physics.nist.gov/PhysRefData/Xcom/html/xcom1.html

[17] G. S. C. Joel, S. Penabei, M. M. Ndontchueng, et al. Precision measurement of radioactivity in gamma-rays spectrometry using two HPGe detectors (BEGe-6530 and GC0818-7600SL models) comparison techniques: Application to the soil measurement. *MethodsX* **4**:42–54, 2017. https://doi.org/10.1016/j.mex.2016.12.003

[18] M. F. L'Annunziata. *Handbook of radioactivity analysis*. Academic Press, 3rd edn., 2012. ISBN 978-0-12-384873-4.

[19] G. F. Knoll. *Radiation detection and measurement*. John Wiley & Sons, Inc., 4th edn., 2010. ISBN 978-0-470-13148-0.

[20] A. Ghalehasadi, S. Ashrafi, D. Alizadeh, N. Meriç. Gamma ray interactions based optimization algorithm: Application in radioisotope identification. *Nuclear Engineering and Technology* **53**(11):3772–3783, 2021. https://doi.org/10.1016/j.net.2021.05.018

[21] S. Ashrafi, O. Jahanbakhsh, D. Alizadeh, B. Salehpour. A novel method for non-destructive Compton scatter imaging based on the genetic algorithm. *Central European Journal of Physics* **11**(5):560–567, 2013. https://doi.org/10.2478/s11534-013-0239-8

[22] Mediasource: CTU through images and sound, 2024. [2024-06-17]. https://media.cvut.cz/en

[23] O. Huml, F. Fejt, J. Rataj. Neutronově-fyzikální charakteristiky AZ C20 školního reaktoru VR-1 [In Czech; Neutron-physical characteristics of the reactor core C20 of the VR-1 training reactor]. Tech. Rep. CTU-14117-P-19-22, KJR FJFI ČVUT v Praze, 2023.

[24] Canberra-Packard. [2024-06-17]. https://www.cpce.net

[25] D. A. Brown, M. B. Chadwick, R. Capote, et al. ENDF/B-VIII.0: The 8^{th} major release of the nuclear reaction data library with CIELO-project cross sections, new standards and thermal scattering data. *Nuclear Data Sheets* **148**:1–142, 2018. https://doi.org/10.1016/j.nds.2018.02.001

[26] The Lund/LBNL nuclear data search. [2024-06-17]. http://nucleardata.nuclear.lu.se/toi/